Tidal Current Measurements Using VHF Radar and ADCP in the Normand Breton Gulf: Comparison of Observations and Numerical Model

Véronique Cochin, *Member, IEEE*, Vincent Mariette, Pierre Broche, and René Garello, *Fellow, IEEE*

***Abstract*—Performance and operational feasibility of very high-frequency (VHF) Doppler radar have been demonstrated in a region dominated by strong tidal currents. An analysis of remote measurements of sea surface currents acquired by Courants de Surface MEsurés par Radar (COSMER)-pulsed Doppler radar during Evaluation et Prévision de l'Environnement Littoral (EPEL) experiment (supported by the French Navy) is presented in this paper. The VHF COSMER radar was deployed to provide continuous sea surface current measurements within an area of about 25 km × 25 km in the Normand Breton Gulf, France. This paper presents VHF measurement comparisons with observations such as acoustic Doppler current profiler (ADCP), as well as comparisons with numerical model TELEMAC 2-D. Results of tidal waves extraction, using harmonic analysis and residual currents, are shown in this paper. We also present a case where radar method is limited, due to the presence of additional peaks in the Doppler spectrum.**

***Index Terms*—Acoustic Doppler current profiler (ADCP), sea measurements, tidal waves, very high-frequency (VHF) pulse Doppler radar.**

I. Introduction

SHORE-based high-frequency (HF) and very high-frequency (VHF) radars (typically between 3–50 MHz) have proved in the last 30 years to be a very useful tool for understanding and analyzing coastal circulation. Radio waves are backscattered by the ocean surface waves and propagation is mainly done by ground-wave propagation. These radar measurements provide quasi-real-time information about oceanographic parameters, such as sea surface currents, sea states, and wind direction, which are calculated using the "Bragg scattering" principle. In operational mode, the radar is at sea level, on the shore.

Crombie [1] first discovered and described the basic physics of the backscattering of radio waves by the ocean surface. The coastal ocean dynamics applications radar (CODAR) system, introduced by Barrick [2] at National Oceanic and Atmospheric Administration (NOAA), has been the first commercial application for mapping surface currents fields. Based on the same technique, other systems have been developed, such as the ocean surface current radar (OSCR) in the United Kingdom [3] or Barrick's SeaSonde in the United States [4]. The University of Hamburg in Germany made experiments with CODAR [5] and developed a new system called Wellen radar (WERA) [6]. Independent of CODAR systems, other developments have been made: high-frequency surface wave radar (HF-SWR) at C-CORE and Northern Radar Systems in Canada [7], PISCES at the University of Birmingham, Birmingham, U.K. [8], VHF Courants de Surface MEsurés par Radar (COSMER) at the University of Toulon in France [9], coastal ocean surface radar (COSRAD) at James Cook University in Australia [10], high-frequency ocean surface radar (HFOSR) at the Okinawa Radio Observatory/ Communications Research Laboratory (ORO/CRL) in Japan [11], multifrequency coastal radar (MCR) at the University of Michigan, Ann Arbor [12], Ocean States Measuring and Analyzing Radar (OSMAR2000) at Wuhan University in China [13] and PortMap at James Cook University in Australia [14].

These systems use different methods to perform spatial resolution both in range and azimuth. Range resolution can be achieved by means of short pulses [2], [3], [9], [10], [12] and frequency-modulated chirps called frequency-modulated continuous wave (FMCW) or frequency-modulated interrupted continuous wave (FMICW) [4], [6]–[8], [11], [13], [14]. Azimuth resolution can be obtained by means of beamforming [3], [6]–[11], [13], [14] and direction-finding (phase comparison) [2], [4], [6], [12]. The working range of HF radars depends on the attenuation of the electromagnetic wave between the transmitter and the target. The attenuation is strongly affected by the condition of sea state (sea too rough or too calm). The attenuation also increases with decreasing seawater conductivity, increasing HF transmitted frequency, increasing distance between the transmitter and the target, and increasing atmospheric noise and/or radio wave interference. A compromise should be found between working range and range resolution, which decreases with decreasing frequency, because of interference

Manuscript received May 23, 2005; accepted September 19, 2006. This work was supported in part by the French Navy [Service Hydrodynamique et Océanographique de la Marine (SHOM)], and by the French Ministry of Research. **Associate Editor: L. R. Wyatt**.

V. Cochin was with the Actimar, Brest, France. She is now with Groupe des Ecoles de Télécommunications (GET), École Nationale Supérieure des Télécommunications (ENST) de Bretagne, Brest Cedex 29238, France (e-mail: veronique.cochin@enst-bretagne.fr).

V. Mariette is with the Actimar, Brest 2920, France (e-mail: mariette@actimar.fr).

P. Broche is with the Laboratoire de Sondages Electromagnétiques de l'Environnement Terrestre, Université du Sud-Toulon-Var, La Garde 83957, France (e-mail: Pierre.Broche@lseet.univ-tln.fr).

R. Garello is with the Groupe des Ecoles de Télécommunications (GET), École Nationale Supérieure des Télécommunications (ENST) de Bretagne, Brest Cedex 29238, France (e-mail: rene.garello@enst-bretagne.fr).

Color versions of one or more of the figures in this paper are available online at http://ieeexplore.ieee.org.

Digital Object Identifier 10.1109/JOE.2006.886077

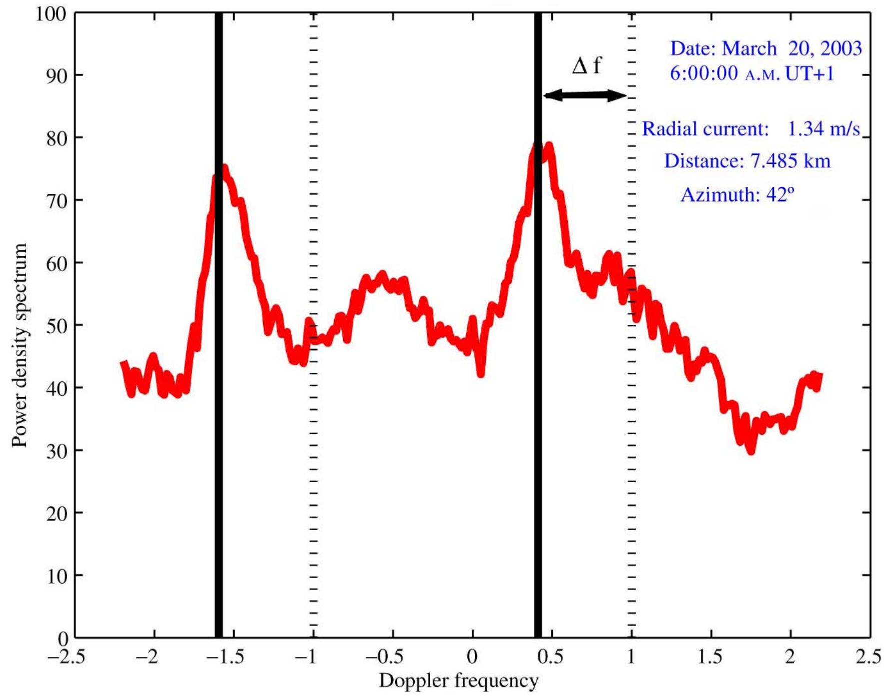

Fig. 1. Sea-echo spectrum from VHF COSMER radar (EPEL program) acquired on March 20, 2003 at 6:00:00 A.M. (UT+1). Bragg peaks are Doppler-shifted away from the theoretical position (normalized Doppler frequency as the x-axis).

from long-range radio sources (transmission from all over the world, reflected by ionosphere). Physical limitations and constraints of performances of HF radars are discussed in [15].

This concept of measurements has received considerable attention in coastal oceanographic experiments to extract ocean parameters [16]. The main advantage of remote sensing methods is to provide real-time measurements with high temporal resolution, over a large scale (thousand of kilometers), which gives the possibility to track oceanographic phenomena. This is not possible with moored instruments such as acoustic Doppler current profiler (ADCP), providing the variation of a parameter with time at a given point. HF radars do not provide a global coverage like the well-known satellite-based systems but they have the advantage to give a continuous observation in limited areas with high spatial resolution (few kilometers down to few hundreds meters) and with high temporal resolution (30 min down to 10 min) in contrast to a repeat cycle of several days for the satellite systems.

This paper presents sea surface current measurements made by VHF COSMER radar set in a strong tidal currents area. Section II describes the HF radar measurement principle and presents the VHF COSMER system, which was used during the Evaluation et Prévision de l'Environnement Littoral (EPEL) experiment. In Section III, we present data analysis and tidal current comparisons between radar measurements, *in situ* data, and numerical simulation. Residual currents and tidal components have been extracted and results are shown.

II. Experiment

A. Radar HF Measurement Principles

Ground-wave radar energy is backscattered from the moving ocean by surface gravity waves. A number of important properties of the ocean wave spectrum can be obtained by looking at the Doppler spectrum of the backscattered signal. Surface ocean currents, waveheights, and wind direction are calculated using the "Bragg scattering" principle [1], [2]. Bragg scattering is a coherent reflection of radio wave energy reflected by ocean surface waves. First-order scatter from specific spectral components of the ocean wavefield produces the dominant contribution. These components, termed "Bragg waves," have a wavelength exactly one-half the transmitted radar wavelength $\lambda_{\rm radar}$ and are moving radially away from or towards the radar. They produce two dominant peaks in the echo Doppler spectrum, symmetrically positioned about the radar frequency. They are displaced according to the phase velocity of the surface waves

$$v_v = \sqrt{\frac{g}{k}} \tag{1}$$

where $k = 2\pi/\lambda$ is the wave number for the ocean waves and g is the acceleration due to gravity. Equation (1) is obtained under the assumption that the ocean depth is greater than half the wavelength of the ocean surface wave.

In the absence of ocean currents, the Doppler frequency shift always occurs at a known position in the frequency spectrum. This frequency depends only on the radar transmitter frequency; it is termed "Bragg frequency"

$$f_B = \sqrt{\frac{g}{\pi\lambda_{\rm radar}}}. \tag{2}$$

If there is a surface current, the returned signal exhibits a Doppler-frequency shift Δf from the theoretical position given in (2). This shift, which is the difference between the theoretical and observed Doppler frequencies, depends on the radial component of the effective surface current moving towards or away from the radar

$$\Delta v = \frac{\lambda_{\rm radar}}{2}\Delta f. \tag{3}$$

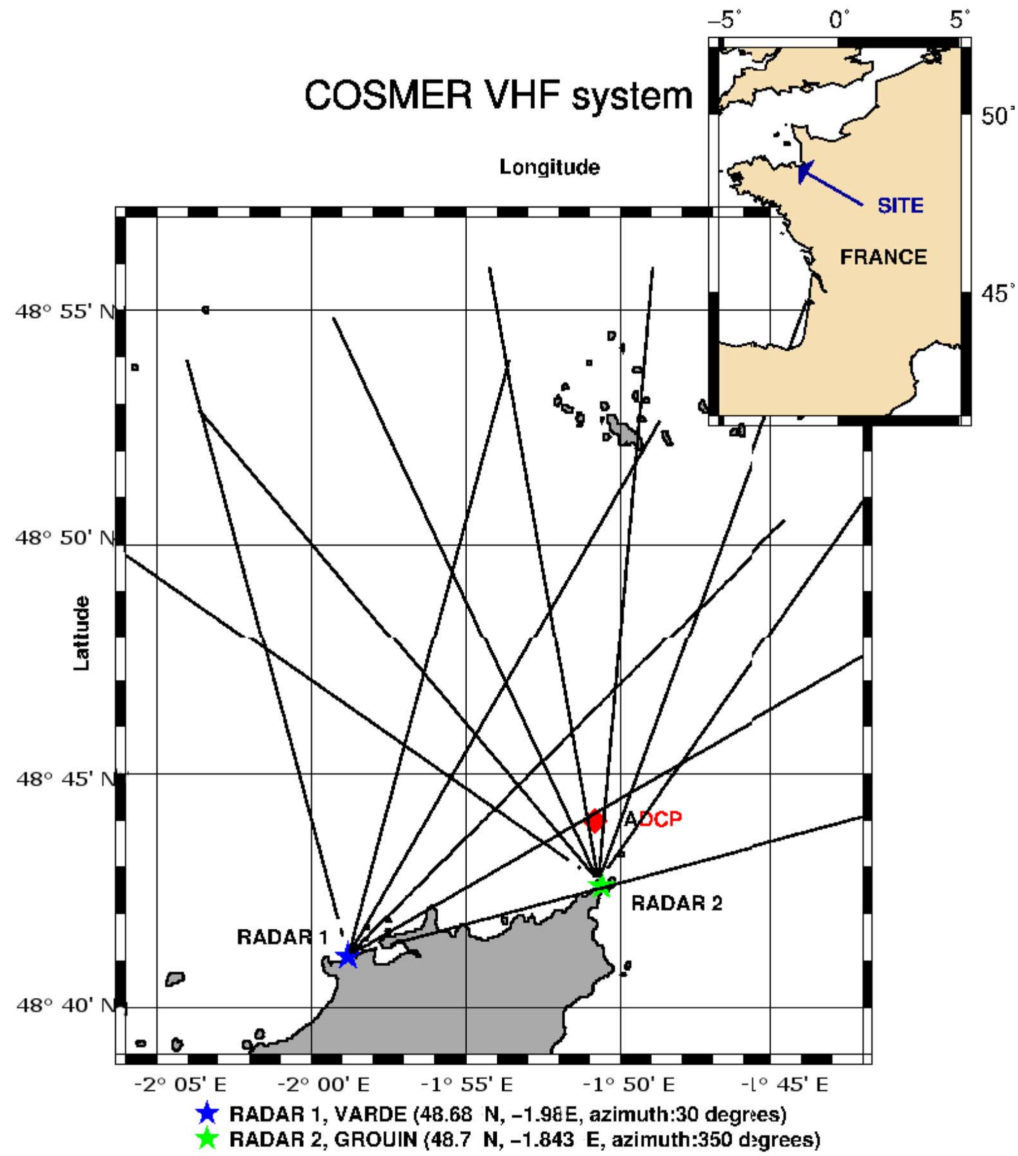

Fig. 2. Site location for VHF COSMER system in Normand Breton Gulf, France, during the EPEL experiment (February–March 2003) and position for the *in situ* instrument (profiler ADCP).

The surface vector current is estimated by combining the components along two radar beams from two separated radar stations. Fig. 1. represents a typical spectrum obtained by VHF COSMER radar during EPEL experiment (45-MHz radar frequency; 6.6-m radar wavelength; 3.3-m Bragg wavelength). First-order lines and Doppler shift Δf are indicated.

The ratio R of energy densities in the two first-order peaks gives information on the wind direction over the ocean [17].

The rest of the power spectrum comprises a continuum referred to as the second-order part of the spectrum and a noise floor. The sidebands surrounding the Bragg peaks are due to nonlinear wave–wave interactions and higher order Bragg scatter. The second-order scatter contains the most significant portion of the ocean wave energy information. Several approaches have been developed to provide a theoretical formulation for relating the Doppler spectrum of the backscatter cross section to the complete ocean wave directional spectrum. Techniques of inversion of the second-order equation are used to extract the two-dimensional (2-D) waveheight spectrum [16].

B. VHF COSMER Radar and ADCP Acquisitions

Data presented here have been acquired during the EPEL experiment at the French coast (Normand Breton Gulf, English Channel) in 2003 with the VHF COSMER system. This experiment "assessment and forecasting of the coastal environment" was supported by the French Navy [Service Hydrodynamique et Océanographique de la Marine (SHOM)]. Performance of VHF COSMER radar, installed for the first time in a region dominated by strong tidal currents (tidal range higher than 10 m) [18], has been evaluated. VHF COSMER system is a radio-oceanographical instrument developed by Laboratoire de Sondages Electromagnétiques de l'Environnement Terrestre (LSEET), University of Sud-Toulon-Var, France [9]. It includes two Doppler radars, set on the coast, operating respectively at

TABLE I
VHF COSMER SYSTEM CHARACTERISTICS IN OPERATIONAL MODE DURING EPEL-GNB PROJECT

Radar COSMER	
Radar type	pulse
Operating frequency	45 MHz / 47.8 MHz
Wavelength	6.66 m / 6.27 m
Length of sea surface wave (Bragg)	3.33 m / 3.13 m
Average power	30 W
Pulse repetition rate	200 µs (5 kHz)
Pulse length	4 µs (possible 1µs)
Radial resolution	600 m (possible 150 m)
Range	30 km
Depth over which current is averaged	0.25 m ($\lambda_{radar}/8\pi$)
Sampling	30 min
Doppler spectrum processing	FFT: 256 points, Sampling frequency: 3 Hz, Frequency resolution 0.01 Hz
Integration time	9 min
Antennas	
Transmit network: **"endfire"**	4 whip antennas $\lambda_{radar}/4$, beam width: 90°(-3 dB)
Receive network: **"broadside"**	8 whip antennas $\lambda_{radar}/4$, (spacing: $\lambda_{radar}/2$)
Azimutal resolution (Beam forming)	+/- 7°(-3 dB)

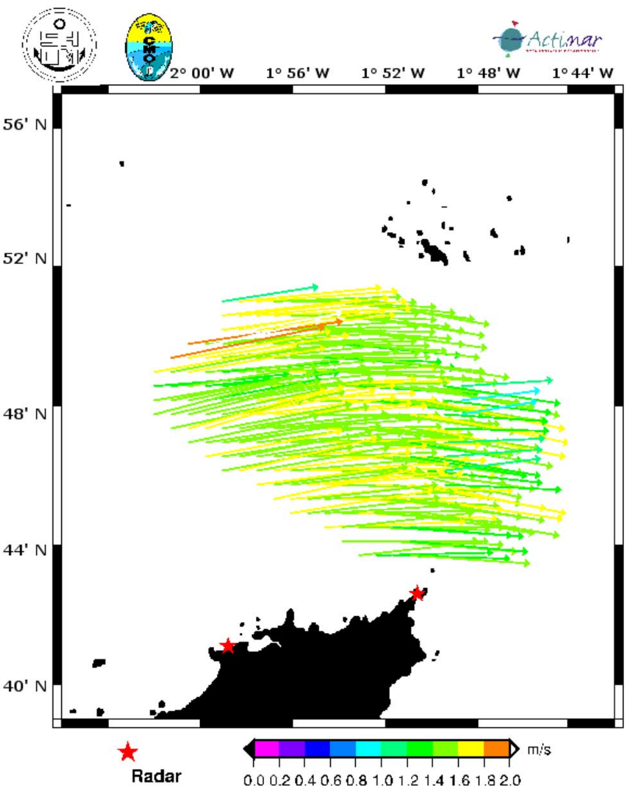

Fig. 3. Current surface mapping by VHF COSMER radar on March 22, 2003 at 08:00:00 P.M. UT+1.

45 and 47.8 MHz. The radars are operated with a linear phased array of eight receive whip antennas parallel to the coast (total length: 25 m or 50 m for 16 antennas), and with a transmitting network of four whip antennas perpendicular to the coast (total length: 12 m). For this experiment, one radar was located at the north of Cancale (Pointe du Grouin, 48° 42′ N, 1° 50′ W) and the other at the north of Saint-Malo (Pointe de la Varde, 48° 41′ N, 1° 58′ W) (see location map on Fig. 2). The radars operate in pulsed mode, with a pulsed width of 4 μs, determining a range resolution of 600 m (possibility of 150 m with this radar) and a pulse repetition rate of 200 μs (maximum range: 30 km).

Both radars measure the radial components of the current in the range direction, at all the sampled distances, with an azimuth resolution of 14° (with eight antennas, beamforming processing). The radar derives vertically averaged quantities over 25 cm (at 50 MHz) and temporally averaged over 9 min. Eastward and northward components of ocean currents are estimated on a 1×1-km^2 grid, combining the radial components along two radar beams. A description of VHF COSMER radar characteristics during the EPEL experiment is given in Table I. Radar measurements were acquired continuously for 28 d, from February 24, 2003 to March 23, 2003, including high spring tide, providing one set of derived parameters (namely an average spectrum) every 30 min. The radar data obtained after real-time signal processing consist of the 256-point Doppler spectra [fast Fourier transform (FFT) algorithm]. These spectra are given for all ranges and azimuth, and are called *radar images*. The database contains 2688 radar images, issued from the two radar stations. Maps of ocean surface currents in the coastal area of about 25 km $\times$ 25 km were sent daily in quasi-real-time on the website of the SHOM throughout the measurement period. Fig. 3 shows an example of sea surface current map as obtained on March 22, 2003 at 08:00:00 P.M. (UT+1), for the maximum flow of spring tide (high water at 11:16:00 P.M., tidal range around 11 m, maximum velocity around 2 m/s). The arrows represent the speed and direction of the surface current velocity. In case of high spring tides, we found strong radial sea surface currents, more than 1.3 m/s, as shown in the Doppler spectrum represented in Fig. 1 (for information, the wave group velocity for Bragg waves, which is the velocity of deep ocean wave packets and also the propagation speed of wave energy, is 1.1 m/s). During this period of high spring tide and strong currents, Doppler spectrum was still measured by the system.

During the experiment, *in situ* instruments such as ADCP and current meters were moored on the bottom of the sea (depth around 20 m). ADCP measurements (48° 44.01′ N, 1° 50.498′ W) were collected from January 8, 2003 to March 10, 2003, at 10-min intervals with an average interval of 2 min. This instrument was adjusted to make Doppler measurements into 28 bins, each with a length of 1 m. Each measurement represents current integrated over two bins (2 m). The vertical profile of the current was also examined, considering all the bins of the ADCP. On spring tide, the sea surface was observed to be above the upper bin (more than 30-m depth), which means that the surface was not detected for some dates (e.g., March 6, 2003). For this analysis, we extracted measurements from a fixed immersion, considering the blind zone of the instrument, which is 4 m below the sea surface.

III. DATA ANALYSIS

To validate VHF radar measurements made in strong tidal areas, we compared several sources of current data: sea surface

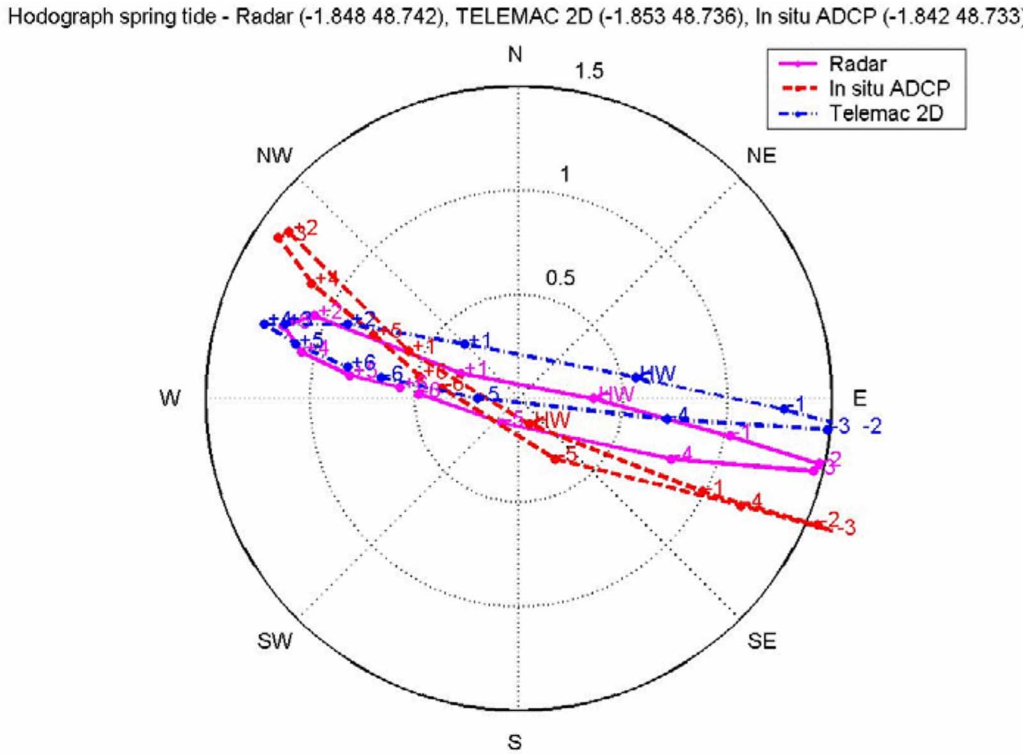

(a)

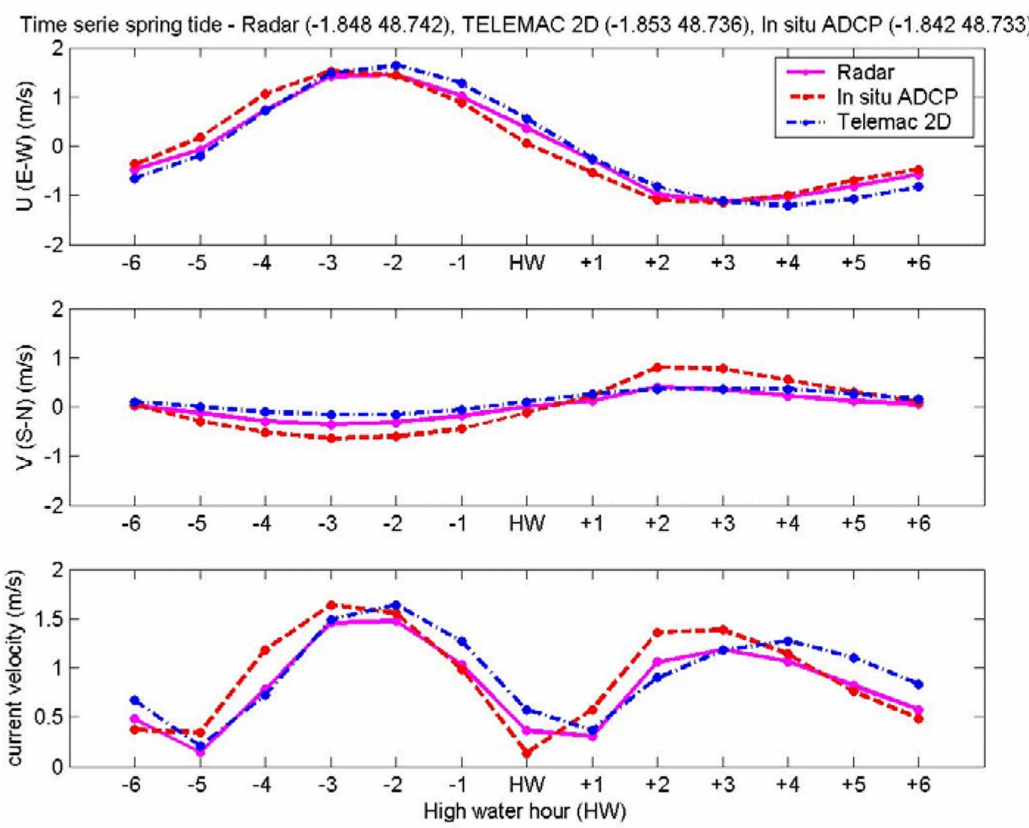

(b)

Fig. 4. Comparisons over the tidal cycle (spring tides, from HW−6 to HW+6) between VHF radar surface currents (line), ADCP measurements (dash line) and TELEMAC 2-D simulations (dot dash line). (a) Hodograph. (b) Time series.

currents, obtained by VHF radar, subsurface currents obtained by ADCP, and simulation from hydrodynamical numerical model TELEMAC 2-D. This model, developed by the Laboratoire National d'Hydraulique et Environnement (EDF-LNHE), France, calculates average currents over the water column on mesh nodes. The simulated surface currents were adjusted to surface current measurements and interpolated on a grid over a spatial resolution of about 1 km in the experiment location. This method is used by SHOM to edit 2-D tidal stream maritime maps [18]. Those maps are useful for navigation. The currents are representative of the tidal current (for a tide cycle, at spring tides and neap tides), but do not take into consideration other physical phenomena, such as wind.

For a fair comparison between the ADCP and radar data, we chose to extract tidal current from measurements. Subtracting mean residual current does this. This current is mainly due to meteorological influence. It is calculated by elimination of surface currents at the tidal frequencies. Statistical analysis of the measurements (total period) over tide cycles is then used: Measurements are brought back to the hour of tide given for the closest reference harbour (St. Malo, France, in this case), using linear interpolation. This allows determining neap tide and spring tide hodographs for measurements. The tidal current vector hodograph is the figure traced out by the tip of a vector representing the current over the tidal cycle, from high water minus 6 h (HW$-$6) to high water plus 6 h (HW$+$6). Fig. 4(a) represents comparisons of hodographs obtained on spring tide for surface currents measured by VHF radar (integration over 0.25 m) and ADCP measurements (integrated over 2 m, at 4-m immersion). Fig. 4(b) gives another representation with time series of the vector currents (U is the east component and V is the north component). These figures show that the maximum currents measured by the instruments have different speed and direction. Observed differences are mainly due to techniques of acquisition [19]. The electromagnetic method yields a spatially and temporally averaged surface current measurement and is limited to observation near the sea surface whereas the acoustic method produces a subsurface point measurement into bins of the water column. Also, higher time integration and temporal resolution might smooth the currents (which can change rapidly, particularly in spring tides). Differences can also been explained by geophysical variability, especially close to the coast (ADCP position), where currents are important and spatially variable (horizontal and vertical). The presence of an island in the area (east of Pointe du Grouin) creates a channel with strong currents during ebb, oriented towards the ADCP position. Those currents are measured by the ADCP (one measurement every 10 min), while the radar measurements smooth them (spatially, over around 1 km^2, and temporally over 9 min, with one measurement every 30 min).

Using a similar algorithm, comparisons between radar measurements and TELEMAC 2-D simulation have been performed for 31 points (radar coverage and SHOM atlas). We found a mean difference of 3 cm/s with a standard deviation of 10 cm/s. The main difference is explained by the technique of acquisition: Numerical model simulations represent estimation of surface currents, with a mean error of 10% whereas radar measurements are surface currents calculated with an accuracy depending on the determination of the center of the Doppler shifted peak. Sea surface current precision is around 2 cm/s for VHF COSMER radar measurements. Fig. 4 also represents an example of hodographs and time series obtained for surface currents measured by VHF radar and TELEMAC 2D over a spring tidal cycle, at the ADCP position.

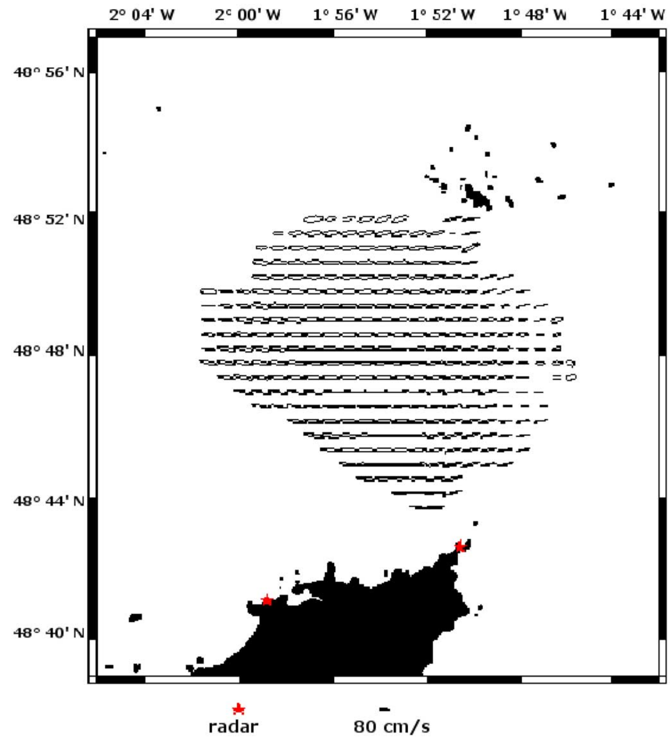

Fig. 5. Tidal ellipses M_2 for VHF radar data over one month measurements (February 24, 2003 at 09:30:00 P.M. to March 24, 2003 at 08:00:00 P.M. UT+1).

Tidal components were extracted from one month measurements by mean of harmonic analysis, based on the least-square method. This is a mathematical process by which the observed tide at any place is separated into basic harmonic constituents. The tools developed at SHOM were used for this analysis. As expected, the semidiurnal M_2 (12.42-h period) tidal component dominates the surface currents, with a mean amplitude of 80 cm/s. Spatially, the M_2 tidal component ellipses were coherent over the VHF radar domain, as shown in Fig. 5, except in an area in the northeast region, classified as "anomalous regions." In this region (see map Fig. 2), certain anomalous behavior in the Doppler spectra appeared, mainly due to sidelobes in antenna pattern and presence of seawater (Mont Saint Michel Bay, France). Examples of Doppler spectrum containing additional (spurious) peaks (energy of Bragg waves seen by the sidelobes antenna pattern) are shown in Fig. 6. Two cases are represented for two closed measurements cells, one with the good Bragg peaks detected, the other with the spurious peaks detected. Nevertheless, the validity of the M_2 tidal component ellipse maps is demonstrated by the comparison we described previously, between the radar measurements and 31 points with known tidal flows in Normand Breton Gulf.

Residual current calculated over several tide cycles and different wind condition periods have been studied. Usually, wind direction is defined as the direction where wind is coming from. Nevertheless, the wind vector in Fig. 7 gives the direction towards which the wind is blowing. In this example, the residual current has been calculated over three tidal periods, having a mean wind direction towards 30° east of north and a mean wind

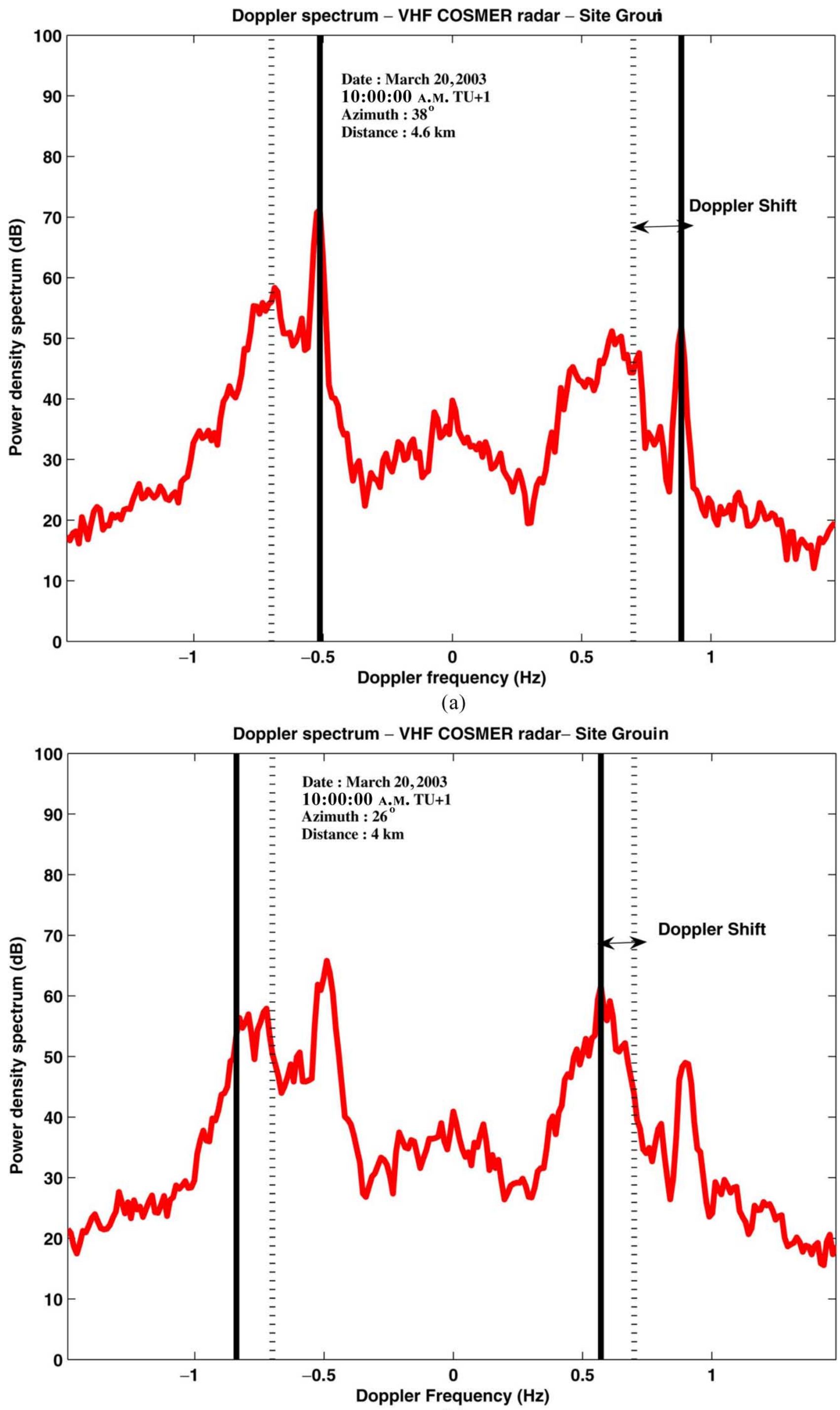

Fig. 6. Doppler spectrum measured by VHF COSMER radar, at the same time, by two closed cells, showing spurious peaks due to sidelobes. Vertical lines represent the selected peaks. (a) Detection of additional peaks. (b) Detection of ”good” peaks.

velocity of 6.4 m/s. Other tests (not shown in this paper) have been made with other wind conditions. This shows that even in strong tidal areas, the influence of meteorological conditions can be seen on residual currents. These surface residual currents are representative of the duration of time measurements, as well as meteorological conditions. To integrate this information in numerical ermodels, it would be important to have larger duration of measurements, which could include more atmospheric variations. At least, one-year duration would be necessary.

IV. CONCLUSION

Performance and operational feasibility of the VHF COSMER Doppler radar have been demonstrated in a region dominated by strong tidal currents. These evaluations proved the capability in mapping coastal ocean surface currents. It also performed the validation of VHF COSMER radar measurements, by comparison with *in situ* instruments and numerical model TELEMAC 2-D. We presented here cases where the radar method is limited.

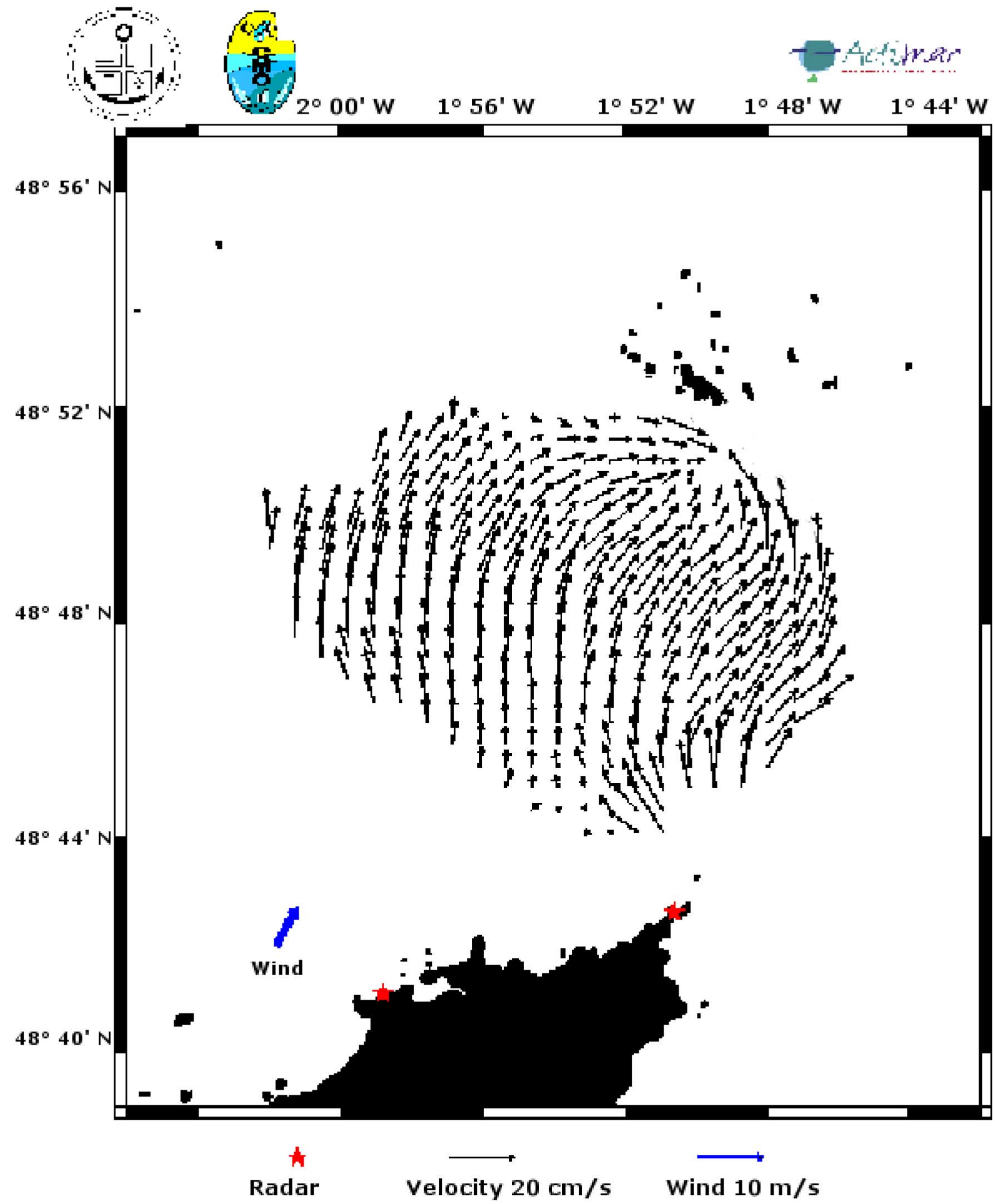

Fig. 7. Eulerien residual current mapping by VHF COSMER radar from March 8, 2003 at 04:00:00 P.M. to March 10, 2003 at 05:30:00 P.M. UT+1. Wind direction (towards 30° east of north) and mean wind velocity (6.4 m/s) are indicated by the arrow (southwest of the map).

The first one is due to the spatial resolution, where measurements are smooth and do not give local strong currents, as shown by the ADCP. This comparison shows the complementarities of both instruments. The second one is due to the presence of spurious peaks in the Doppler spectrum. Those peaks represent energy stronger from the Bragg waves in the direction of the sidelobes in antenna pattern (presence of seawater), than those from the principal radar beam (in some case of wind and current conditions). Time-frequency analysis on the whole duration of the signal or unmixed processing could be applied to eliminate spurious peaks. We also showed that extraction of tidal components can be done, by the same process as for *in situ* instruments, within a large area. Tidal ellipses are particularly useful for calibrating the numerical models. Radar measurements are also used to increase the precision of the coastal hydrodynamic models by means of data assimilation. These measurements also have an important role in term of operational surveillance, because of their high temporal resolution (every 30 min, down to 10 min) and large-scale domain, which offer good opportunity for control and operational surveys.

ACKNOWLEDGMENT

The authors would like to thank SHOM and particularly F. Ardhuin, A. Pichon, R. Le Roy, B. Simon, L. Pineau, M. Le Goff, and M. Aidonidis for providing data sets and support in performing some of the harmonic analysis. Tidal components and statistic analysis were extracted using software developed at SHOM. The authors would also like to thank LSEET group, particularly J. Gaggelli, Y. Barbin, J. C. de Maistre, and P. Forget, for help in collecting the VHF COSMER data, A. Coat of Actimar and G. Mercier of GET-ENST for help in data processing, and Conservatoire de l'espace littoral et des rivages lacustres, Conseil général de l'Ille et Vilaine, and local authorities for authorization in radar settings.

REFERENCES

[1] D. Crombie, "Doppler spectrum at sea echo at 13.56 Mc/s," *Nature*, vol. 175, pp. 681–682, 1955.

[2] D. E. Barrick, M. W. Evans, and B. Weber, "Ocean surface currents mapped by radar," *Science*, vol. 198, pp. 138–144, 1977.

[3] D. Prandle, S. G. Loch, and R. J. Player, "Tidal flow through the Straits of Dover," *J. Phys. Oceanogr.*, vol. 23, no. 1, pp. 23–37, 1993.

[4] J. D. Paduan and L. K. Rosenfeld, "Remotely sensed surface currents in Monterey Bay from shore-based HF radar (CODAR)," *J. Geophys. Res.*, vol. 101, no. C9, pp. 20 669–20 686, 1996.

[5] K. W. Gurgel, H. H. Essen, and F. Schirmer, "CODAR in Germany—A status report valid November 1985," *IEEE J. Ocean. Eng.*, vol. 11, no. 2, pp. 251–257, Apr. 1986.

[6] K. W. Gurgel, G. Antonischki, H. H. Essen, and T. Schlick, "Wellen radar (WERA), a new ground-wave based HF radar for ocean remote sensing," *Coastal Eng.*, vol. 37, no. 3-4, pp. 219–234, 1999.

[7] K. Hickey, R. H. Khan, and J. Walsh, "Parametric estimation of ocean surface currents with HF radar," *IEEE J. Ocean. Eng.*, vol. 20, no. 2, pp. 139–144, Apr. 1995.

[8] E. D. Shearman and M. D. Moorhead, "PISCES: A coastal ground-wave radar for current, wind and wave mapping to 200 km ranges," *Proc. Int. Geosci. Remote Sens. Symp. (IGARSS)*, pp. 773–776, 1988.

[9] P. Broche, J. C. Crochet, J. C. de Maistre, and P. Forget, "VHF radar for ocean surface current and sea state remote sensing," *Radio Sci.*, vol. 22, pp. 69–75, 1987.

[10] M. L. Heron, P. E. Dexter, and B. T. McGann, "Parameters of the air-sea interface by high-frequency ground-wave HF Doppler radar," *Aust. J. Mar. Freshwater Res.*, vol. 36, pp. 655–670, 1985.

[11] H. Takeoka, Y. Tanaka, Y. Ohno, Y. Hisaki, A. Nadai, and H. Kuroiwa, "Observation of the Kyucho in the Bungo Channel by HF radar," *J. Oceanogr.*, vol. 51, no. 6, pp. 699–711, 1995.

[12] C. C. Teague, J. F. Vesecky, and Z. R. Hallock, "A comparison of multi-frequency HF radar and ADCP measurements of near-surface currents during COPE-3," *IEEE J. Ocean. Eng.*, vol. 26, no. 3, pp. 399–405, Jul. 2001.

[13] W. Huang, S. Wu, E. Gill, B. Wen, and J. Hou, "HF radar wave and wind measurement over the Eastern China Sea," *IEEE Trans. Geosci. Remote Sens.*, vol. 40, no. 9, pp. 1950–1955, Sep. 2002.

[14] M. L. Heron, T. Helzel, A. Prytz, M. Kniephoff, and W. J. Skirving, "PortMap: A VHF ocean surface radar for high spatial resolution," *Proc. IEEE OCEANS—Europe*, vol. 1, pp. 511–515, 2005.

[15] K. W. Gurgel, H. H. Essen, and S. P. Kingsley, "High frequency radars: Physical limitations and recent developments," *Coastal Eng.*, vol. 37, no. 3-4, pp. 201–218, 1999.

[16] L. R. Wyatt, "Limits to the inversion of HF radar backscatter for ocean wave measurement," *J. Atmos. Ocean. Technol.*, vol. 17, pp. 1651–1665, 2000.

[17] M. L. Heron and R. J. Rose, "On the application of HF ocean radar to the observation of temporal and spatial changes in wind direction," *IEEE J. Ocean. Eng.*, vol. 11, no. 2, pp. 210–218, Apr. 1986.

[18] Service Hydrographique et OcéAnographique de la Marine: Courants de Marée dans le Golfe Normand Breton de Cherbourg à Paimpol 1998.

[19] H. C. Graber, B. K. Haus, R. D. Chapman, and L. K. Shay, "HF radar comparisons with moored estimates of current speed and direction: Expected differences and implications," *J. Geophys. Res.*, vol. 102, no. C8, pp. 18749–18766, 1997.

Véronique Cochin (M'03) was born in 1972. She received the engineering degree in 2002 and the Ph.D. degree in signal processing and telecommunications in 2006, both from the Ecole Nationale Supérieure des Télécommunications de Bretagne (ENST Bretagne), Brest, France. Her thesis was focused on the evaluation of the HF/VHF coastal radars for operational oceanography, particularly in Brittany, France, areas with strong tidal currents and high variability.

Vincent Mariette was born in 1952. He received the Ph.D. degree in physical oceanography from The Université de Bretagne Occidentale, Brest, France, in 1983.

From 1978 to 1987, he was a Researcher at the Centre National de la Recherche Scientifique (CNRS), Laboratoire de Physique des Océans, Brest, France. In 1987, he founded a marine farm, and worked for ten years as a shell fisherman. In 1997, he founded a private company Actimar, Brest, France, which focused on operational oceanography.

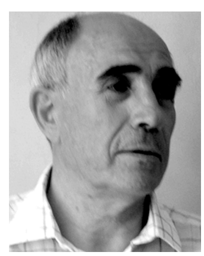

Pierre Broche received the M.S. degree in physics from École Normale Supérieure, Paris, France, in 1965 and the Ph.D. degree from Faculté des Sciences de Paris, Université Paris, Paris, France, in 1969.

He is currently a Professor at the Université de Toulon et du Var, La Garde, France. He has over 30 years experience in radar remote sensing of the sea surface and its application for coastal studies (wind waves and currents, river plumes, etc.).

René Garello (M'85–SM'96–F'06) was born in 1953. He received the Ph.D. degree in signal processing from the Institut National Polytechnique de Grenoble (INPG), Grenoble, France, in 1981. In 1995, he received the Habilitation to Supervise Research (HDR).

From 1982 to 1984, he worked as a Research Associate at Aeronomy Lab, National Oceanic and Atmospheric Administration (NOAA), Boulder, CO. He joined the Ecole Nationale Supérieure des Télécommunications de Bretagne (ENST Bretagne), Brest, France, in 1985, where in 1988, he became a Professor in the field of signal processing and image processing. He has supervised about 20 Ph.D. students and reviewed about 20 Ph.D. or HDR theses. He coauthored 30 papers in peer-reviewed journals, three books, and near 100 communications in international conferences. He is a peer reviewer for about ten scientific international journals and international applications (European Union, Norway, Canada). He is involved with the research structure at Groupe des Ecoles des Télécommunications (GET), ENST, Brest, France, and supervises the theme "Environment." He is the Head of the team "Information Processing for Oceans and Environment" in the Centre National de la Recherche Scientifique (CNRS) research lab associated with GET—ENST Bretagne.

Dr. Garello has been an Associate Editor for Region 8 of the IEEE JOURNAL OF OCEANIC ENGINEERING since 1997. He received the "Palmes Académiques" in 2002 for all his activities within the GET.